Chapter 20

Magic Angle Spinning Nuclear Magnetic Resonance of the Chlorosomes

Ido de Boer and Huub J. M. de Groot*
Leiden Institute of Chemistry, Einsteinweg 55, P.O. Box 9502, 2300 RA Leiden, The Netherlands

Summary

Chlorosomes, the oblong light-harvesting bodies of green photosynthetic bacteria, are attached to the inner side of the cytoplasmic membrane. Magic Angle Spinning Nuclear Magnetic Resonance (MAS NMR) was used to study isotopically labeled chlorosomes and in vitro model compounds. Using uniform isotope labeling of chlorophyll molecules, 2D and 3D MAS NMR dipolar correlation spectroscopy was performed in high magnetic field. The chemical shifts provided invaluable information about the structure via ring current effects, while long range correlations were generated that lead to intermolecular distance constraints. Novel methodology was developed and implemented using a Chl *a*/H_2O aggregate, and a structural arrangement of bilayers of Chl sheets with interdigitating tails was resolved. Application of this technology to chlorosomes and BChl *c* aggregates provided unambiguous evidence that self-organization of BChl *c* is the principal structural factor in establishing the rod elements in chlorosomes. This confirms that proteins do not play an essential role in the light harvesting function, which is of fundamental biological interest. Finally, MAS NMR leads to a bilayer model for the tubular supra-structure of sheets of BChl *c* in the chlorosomes of *Chlorobium tepidum*.

Note: Readers are encouraged to visit the website (http://epub.ub.uni-muenchen.de/archive/00000776/) for 'supplementary material,' where Figs. S1–S2 referred to in the text are posted.

I. Introduction

Chlorosomes are found in photosynthetic green bacteria as ellipsoid vesicles of about 100–300 nm in length attached to the inner surface of the cytoplasmic membrane, where they provide a large cross-section for the absorption of sunlight (Blankenship et al., 1995; Olson, 1998). The chlorosomes contain rod-shaped elements of 5 nm in diameter for *Chloroflexus* (*Cfl.*) and 10 nm for *Chlorobium* (*Chl.*)

*Author for correspondence, email: groot_h@chem.leidenuniv.nl

Bernhard Grimm, Robert J. Porra, Wolfhart Rüdiger and Hugo Scheer (eds): Chlorophylls and Bacteriochlorophylls: Biochemistry, Biophysics, Functions and Applications, pp. 297–307.

as visualized by electron microscopy (Staehelin et al., 1978, 1980). The assumption that the rods are formed by protein-pigment complexes, as found in other photosynthetic elements, has been challenged by increasing evidence that self-organized bacteriochlorophyll (BChl) *c* is responsible for the shape and function of the antennae. The crucial evidence is that the in vitro aggregation of BChl *c* leads to similar structures and spectroscopic properties as occur in the natural system (for review, see Tamiaki et al., 2002). Small-angle neutron scattering studies have indicated cylindrical shaped micelles for aggregates prepared in organic media (Worcester et al., 1986). In addition, various spectroscopic methods suggest a highly ordered structure of both aggregated BChl *c* and the chlorosomes (Griebenow et al., 1991; Matsuura et al., 1993; Hildebrandt et al., 1994). Molecular modeling has also been used to explain the structural features of the cylindrical micelles (Holzwarth and Schaffner, 1994). For the chlorosomes, an intermolecular bonding network has been proposed, where the 3^1-hydroxy group of BChl *c* coordinates to the central metal of a neighboring BChl *c* molecule and also hydrogen bonds with the 13^1 carbonyl-oxygen of yet another BChl molecule (Holzwarth and Schaffner, 1994; Chiefari et al., 1995).

In the past, NMR has contributed significantly to the study of chlorophyll chemistry, which was reviewed extensively (Abraham and Rowan, 1991). Two different routes have been worked out to use NMR data for structure determination in uniformly ^{13}C-labeled chlorophylls. Firstly, the chemical shift assignment obtained from correlation experiments can provide information about the spatial structure. This is consistent with the early analyses of the stacking in small chlorophyll aggregates from ring current shifts (Abraham and Rowan, 1991). In particular, ^{1}H aggregation shifts are important for the purpose of structure determination. The chemical shift of ^{1}H is relatively insensitive to electronic perturbations, while shifts induced by ring currents are large on the ^{1}H shift scale of 10–15 ppm. In a similar way, the ring current shifts are indispensable for structure elucidation in the solid state. Secondly, structural information in the solid state may be obtained from the measurement of distance restraints revealing close contacts between molecular moieties.

In this Chapter, recent progress in resolving the nature of the chlorosomal antennae that has been acquired by magic angle spinning (MAS) NMR studies is discussed. The structure elucidation strategy using a chlorophyll (Chl) *a*/H_2O model system is summarized and the MAS NMR investigations of the chlorosomes are reviewed. It has been found that the chlorosomes consist mainly of aggregated BChl that is indistinguishable from BChl *c* precipitated from hexane. Based on MAS NMR experiments, a bilayer tube model for the chlorosomes has been proposed.

II. Aggregated Hydrated Chlorophyll (Chl *a*/H_2O) as a Model for Magic Angle Spinning Nuclear Magnetic Resonance Technology Development

Much of the MAS NMR methodology was first tested using a Chl *a*/H_2O aggregate and then applied in a second step to study the structure of the chlorosomes. The Chl *a*/H_2O aggregate is very suitable to develop and evaluate novel pulse sequences. As a moderately-sized molecular system, it represents an intermediate between small model compounds, such as the tyrosine HCl salt, that are frequently used for a demonstration of principles of pulse techniques, and larger systems of genuine biological interest. The chemical structure of Chl *a* is depicted in Fig. 1. The aggregation of Chl *a* and the Chl-water interaction in Chl *a*/H_2O micelles has been extensively studied in the past (Katz et al., 1991). Chl *a* can only form solid aggregates by incorporation of H_2O, which is believed to coordinate the central magnesium atom and form hydrogen bonds with the carbonyl functions of surrounding molecules. Recent MAS NMR results suggest a close homology between the structure of Chl *a*/H_2O and crystalline ethyl-chlorophyllide *a*, with two water molecules forming the bridging network (Boender et al., 1995; de Boer et al., 2002; van Rossum et al., 2002).

Complete ^{1}H and ^{13}C assignments were obtained in a field of 14.1 T using the ^{13}C-^{13}C radio frequency-driven dipolar recoupling (RFDR) and ^{1}H-^{13}C Lee Goldburg/cross polarization (LG-CP) methods (van Rossum et al., 2002) (see Table S1 in Supplementary Material). The line widths are small (120–200 Hz) revealing a rigid and well-ordered structure. The ^{1}H and ^{13}C shifts of the monomer in solution were used

Abbreviations: BChl – bacteriochlorophyll; *Cfl.* – *Chloroflexus*; Chl – chlorophyll; *Chl.* – *Chlorobium*; CP – cross polarization; CS – chemical shift; LG – Lee Goldburg; MAS – magic angle spinning; NMR – nuclear magnetic resonance; RFDR – radio frequency-driven dipolar recoupling; WISE – wideline separation

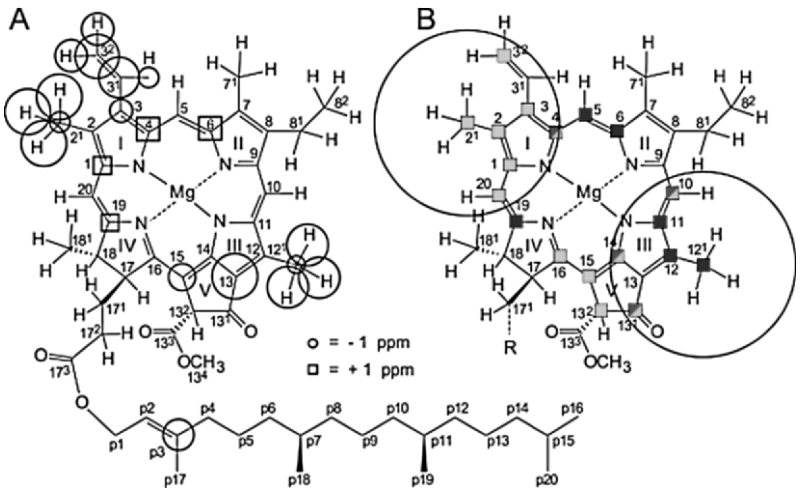

Fig. 1. (A) Visual representation of the carbon and proton aggregation shifts ($\Delta\sigma$) for aggregated Chl *a*. The circles around the carbon and hydrogen atoms represent upfield aggregation shifts, squares represent downfield shifts. The sizes of the circles and squares reflect the magnitude of the aggregation shifts. (B) Schematic representation of the assignment of heteronuclear correlations involving the 2^1-H_3, which are shown in shaded grey or the 12^1-H_3, which are solid black. For the 4-C, 10-C, 13^1-C and 14-C the correlations with proton signals are assigned to transfer from both methyl groups. The ranges for intramolecular transfer for the two methyl groups are indicated with the circles. Intramolecular correlations involving the 3^1-C and 13-C could not be assigned. Reprinted from Van Rossum et al. (2002). Copyright (2002), with permission from Elsevier.

to estimate the aggregation shifts. The ^{1}H aggregation shifts are consistent with the pattern for ^{13}C (Fig. 1). Upfield aggregation shifts up to ~5 ppm are observed, mostly induced by ring currents. The shift pattern is in agreement with models for the Chl *a*/water aggregates that assume strong overlap between the rings A and the rings C and E of adjacent molecules forming stacks (Worcester et al., 1986). In addition, in a 2D ^{13}C-^{13}C RFDR spectrum recorded with a long mixing time of τ_m = 10 ms, several cross-peaks are observed that can be attributed to intermolecular transfer (Boender et al., 1995).

Heteronuclear ^{1}H-^{13}C spectra were recorded with long LG-CP times to generate intermolecular correlations (van Rossum et al., 2002). For a LG-CP time of 2 ms, a maximum transfer distance (d_{max}) of ~4.2 Å was estimated from an analysis of the correlations involving the 2^1-H_3 and 12^1-H_3 protons. Weak transfer was observed from the 2^1-H_3 protons to the 10, 13^1, 13^2, 14, 15 and 16 carbons at the opposite side of the molecule (Fig. 1B), which was assigned to intermolecular contact over distances ~4 Å. Similarly, weak correlations between the 12^1-H_3 protons and the 4, 5, 6 and 19 carbons indicate intermolecular transfer. They confirm the 2D arrangement of the Chl *a* in sheets (Fig. 3A).

In addition, a CP^3 experiment can provide intermolecular ^{13}C-^{13}C correlations employing mixing by ^{1}H spin diffusion. An example of a CP^3 experiment, using a short mixing time of 0.1 ms, is shown in

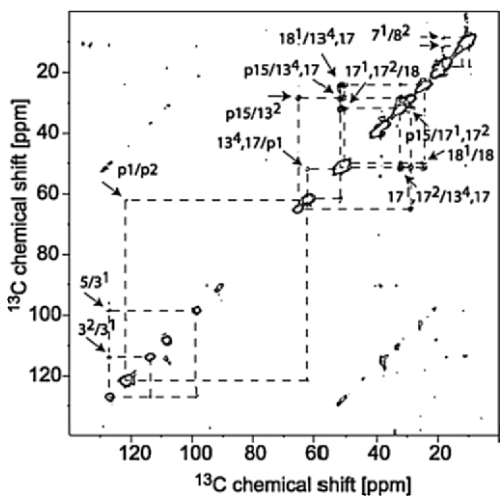

Fig. 2. Contour plot of an absorption mode 2D ^{13}C-^{13}C CP^3 MAS NMR correlation spectrum of aggregated Chl *a*/H_2O recorded with a spinning speed of 14.5 kHz in a field of 17.6 T. Arrows and labels are used to indicate cross-peaks, which are connected to the corresponding diagonal peaks and mirror peaks by dashed lines. Data were acquired with τ_m = 100 µs. A prescan delay of 1 s was used for a total of 192 scans for each of 200 t_1 points.

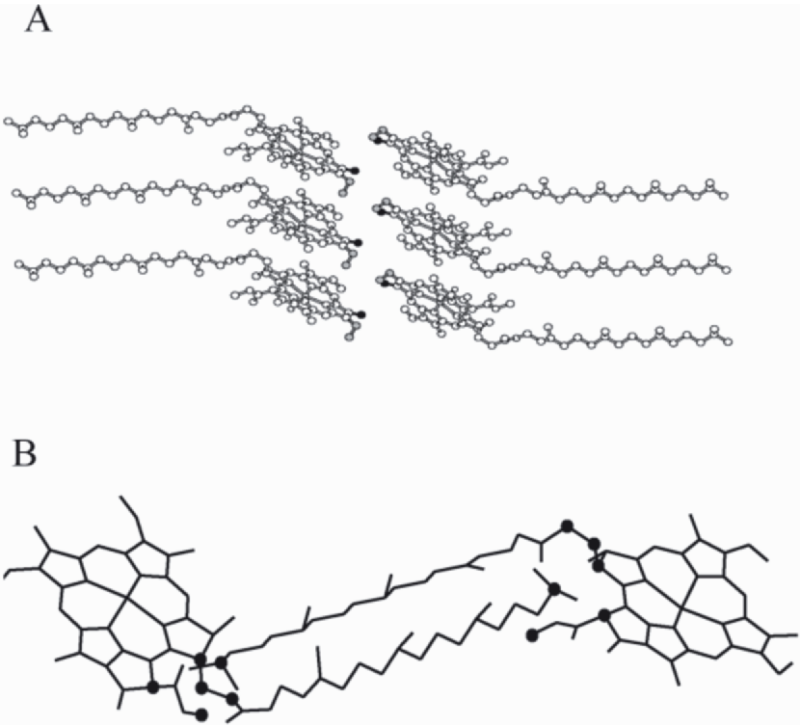

Fig. 3. (A) Schematic representation of a bilayer formed from two sheets of microcrystalline aggregated Chl *a*/H_2O. The orientation of the 2-D sheets is perpendicular to the plane of the paper and the view is parallel to the stack. The 7-Me and 8-Et moieties are shown in black and grey, respectively. (B) The proposed structural arrangement of the two Chl *a* molecules in the unit cell. Solid circles indicate the carbons involved in the intermolecular correlations.

Fig. 2 (de Boer et al., 2002). Correlations between the P15 carbon at the end of the phytyl chain and the 17^1, 17^2, 13^2 and 13^4 carbons near the base of the tail are observed. From a series of experiments using increasing mixing times, it is estimated that d_{max} is about ~4 Å for a mixing time of 0.1 ms. The length of the phytyl tail is ~20 Å, much longer than d_{max} and hence the correlations involving P15 are attributed to intermolecular transfer, over distances no larger than ~4 Å. This leads to the bilayer model with stretched and inter-digitating tails (Fig 3B). This model is supported by the very modest inhomogeneous line broadening for the phytyl tails and the absence of aggregation shifts for the tails, which provides strong evidence that the tails have essentially the same conformation as in solution.

Finally, ^{1}H signals, correlating with similar bridging moieties in the heteronuclear MAS NMR spectra, could be assigned to structural water similar to ethylchlorophyllide *a*. In addition, a small doubling of the 7-C, 7^1-CH_3 and $8^{1,2}$-C was resolved. This provides evidence for two marginally different well-defined molecular environments at the interface between two bilayers (Fig. 3A).

III. Self-organization of Bacteriochlorophyll is the Main Structural Feature of the Chlorosomal Antennae

A complete ^{13}C assignment was made for the NMR response of the chlorosomes and various BChl *c* homologues from the uniformly ^{13}C labeled chlorosomes of *Chl. tepidum* (Balaban et al., 1995) (see Table S2 in Supplementary Material). Figure 4 shows the chemical structure of the most abundant [8-Et, 12-Et]BChl *c* homologue. 2D ^{13}C-^{13}C RFDR dipolar correlation spectra of solid BChl *c* aggregated in hexane and the chlorosomal antennae are depicted in Fig. 5 (Balaban et al., 1995; Boender, 1996). Many peaks are resolved in the spectra, and the two spectra are almost identical. The predominant component of the MAS NMR signals in the chlorosomes is from BChl *c*. Only a minor fraction is observed in the chlorosomes that is not present in the aggregate. These peaks are attributed to lipids and proteins in the chlorosomes. Correlations between the carbonyl and α carbons of a small protein component are indicated in Fig 5.

The 2D response of the BChl *c* in intact chlorosomes is virtually indistinguishable from the data

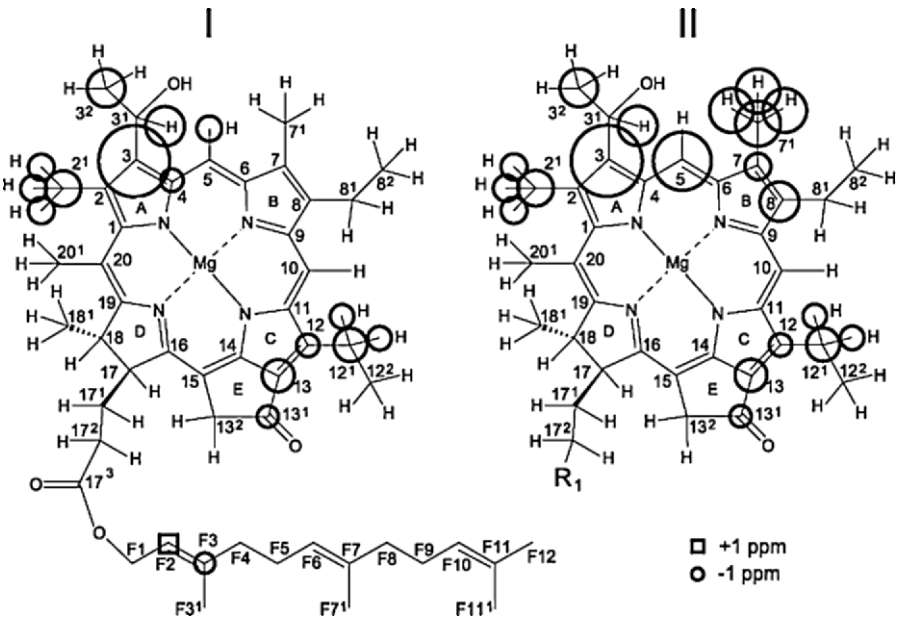

Fig. 4. Carbon and proton aggregation shifts $|\Delta\sigma_i| \geq 1.5$ ppm of BChl *c* with $\Delta\sigma_i = \sigma_i - \sigma_{liq}$. The NMR response comprises two components, denoted **I** and **II**. The circles around the carbon and hydrogen atoms represent upfield aggregation shifts, the squares downfield aggregation shifts. The size of a circle or square is proportional to the magnitude of the aggregation shift. Reprinted with permission from Van Rossum et al. (2001). Copyright (2001) Am. Chem. Soc.

collected from the in vitro aggregate with respect to chemical shifts, line widths and relative intensities of the cross-peaks. This demonstrates that the minor fractions of proteins and lipids are not an integral part of the BChl *c* assembly (Balaban et al., 1995; Boender, 1996). In this way, the NMR data provide conclusive evidence that self-assembly of BChl *c* is the structural basis for the BChl *c* organization in vivo, without the intervention of proteins.

In earlier 1D MAS NMR experiments, solid BChl *c* was also compared with the chlorosomes, providing the first evidence for the same aggregated forms (Nozawa et al., 1990, 1991, 1994). The T_{CH} and $T_{1\rho}{}^{H}$ values were also comparable for both samples, which corroborates the structural correspondence between the aggregate and the natural system.

The observation that a biological function can be realized without active participation of protein can be considered anomalous, since the central dogma of molecular biology states that all function originates from the DNA code via protein: DNA → RNA → protein → function. In a chlorosome, the biological function of the antennae is based on self-assembly steered by the physico-chemical properties of the constituting molecules and top-down control from higher levels in the biological hierarchy. Other examples of this principle have been encountered in the past, such as biomineralization of inorganic matter into a morphology controlled by the organism (Bäuerlein, 2003). For instance, the magnetite crystals in the magnetosomes of magnetobacteria correspond to single magnetic domains of 40–120 nm, and allow the bacteria to orient themselves using the earth magnetic field.

The self-organization of BChl *c* may be of interest for artificial photosynthesis. The elucidation of the functional concepts behind photosynthesis in nature is expected to be of assistance in improving artificial devices like photovoltaic cells. Although the actual application of artificial molecular solar energy converters may still be years away, elucidation of the concepts behind nature's efficient energy converting system will be of use to photovoltaics and molecular electronics research. In particular, the discovery of natural light-harvesting systems without proteins may be of help to indicate novel routes in photovoltaics research.

To produce aggregates resembling the chlorosomes, the solvent used in the process is essential. In particular, the effect of different solvents to form

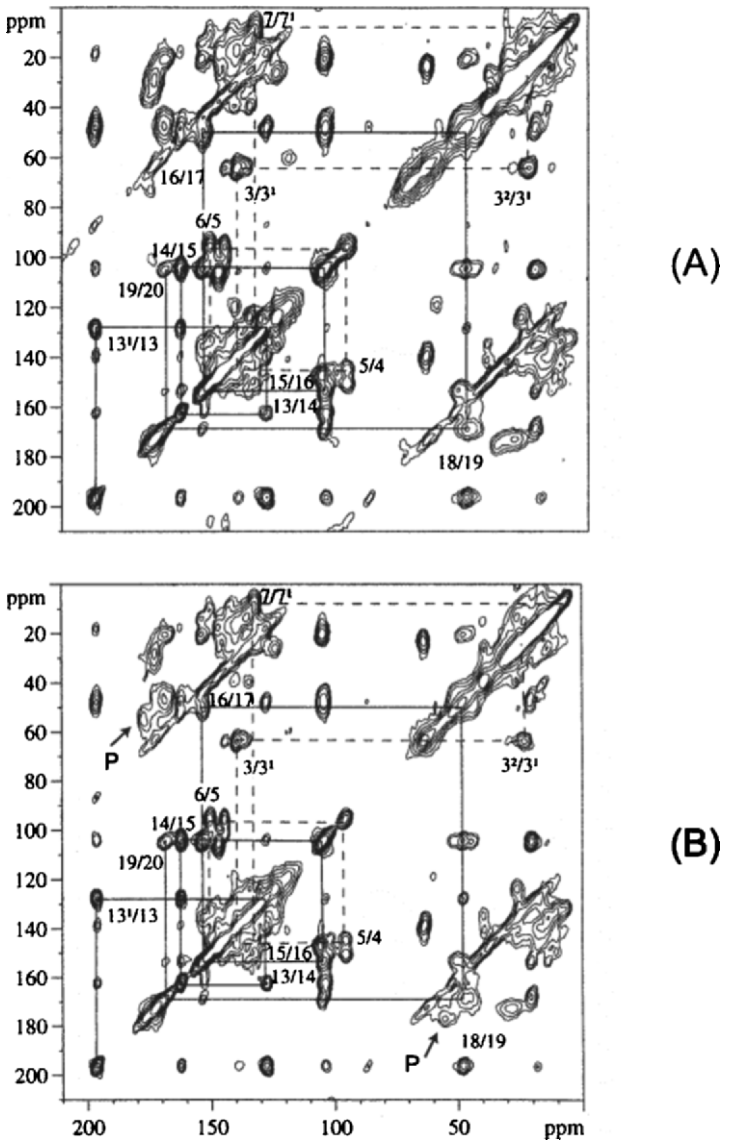

Fig. 5. Contour plots of 2D MAS NMR dipolar correlation NMR spectra of uniformly ^{13}C labeled BChl *c* aggregates (A) and ^{13}C labeled chlorosomes (B), recorded in a magnetic field of 9.4 T. The MAS rate was 11 kHz and a CP time of 1 ms was used. The lines indicate sequences of nearest neighbor correlations. A small protein fraction in (B) is indicated with P. Reprinted from Boender (1996).

solid aggregates of (3¹ *R*) BChl *c* was recently studied (Umetsu et al., 1999). Various techniques including ^{13}C CP/MAS were applied to investigate the size and order of the aggregates formed after drying in diethyl ether, CH_2Cl_2, CCl_4 or CH_2Cl_2 in an excess of hexane. From the magnetic circular dichroism spectra, the aggregates treated with CCl_4 and hexane were estimated to be larger than those with diethyl ether and CH_2Cl_2. The circular dichroism spectra show differences between the CH_2Cl_2-treated aggregates and the diethyl ether and CCl_4-treated samples, indicating a different molecular arrangement. In addition, the BChl *c* treated with CH_2Cl_2 is weakly diffracting by X-ray similar to methyl-BChlide *c* formed in hexane. This shows that the tails leave the stacking of the BChl *c* intact. In addition, recent MAS NMR experiments revealed two distinct sets of resonances for a CH_2Cl_2-treated uniformly ^{13}C and ^{15}N labeled (3¹ *R*) BChl *c* aggregate, indicating the formation of a transient species between the dimer and the stacked form (Umetsu et al., 2004).

IV. A 3-Dimensional Model for the Structure of the Chlorosomal Antennae

The structure of the chlorosomal antennae was recently investigated with 2D and 3D MAS NMR. The ^{13}C shifts assigned from the 2D RFDR experiments provided the first step to a structural model (Balaban et al., 1995). The relatively large ^{13}C line widths contrast with the microcrystalline Chl *a*/H_2O aggregates and reveal significant disorder down to the microscopic level. Large ring current shifts are detected in the regions of rings A, -C and E (Fig. 4). ^{13}C-^{13}C RFDR experiments were performed, using long mixing times of 5–10 ms (Boender, 1996; van Rossum et al., 1998a). Correlations between the 13^1-carbon and the 19-, 20-, 1-, 2- and 3-carbons were attributed to intermolecular transfer and appear to confirm the layer structure. In addition, rotational resonance experiments show that the $C3^1$-$C13^1$ distance is similar to the C20-$C3^1$ distance in accordance with hydrogen bonding between the 3^1 and 13^1 groups (Nozawa et al., 1994).

The ^1H shifts were determined in a 3D experiment using rapid MAS in combination with a high magnetic field. Under these conditions, it was shown that proton shifts can be determined and intermolecular heteronuclear correlations as well as hydrogen–bonding characteristics can already be determined with simple pulse schemes such as the wideline separation (WISE) technique (van Rossum et al., 1996). Since the chlorosome response is considerably inhomogeneously broadened, a 2D ^{13}C-^{13}C RFDR experiment was extended in a straightforward fashion by a third ^1H WISE dimension to construct a 3D ^1H-^{13}C-^{13}C MAS NMR experiment (van Rossum et al., 2001). As a result, all ^1H resonances of the chlorosomes could be assigned (see Table S2 in Supplementary Material). The aggregation shifts (Fig. 4) are consistent with the ^{13}C pattern. Two fractions **I** and **II** are observed in the NMR dataset. In both fractions, two regions with pronounced upfield shifts are visible around ring A and C/E. In addition, in fraction **II**, large upfield shifts for the 5-C and the 7-Me are detected. This suggests the existence of two distinct structural arrangements, related to the rod-like suprastructure in the chlorosomes.

The chemical shift data were used to refine the structural model for the chlorosomes. Firstly, the molecular structure was optimized by quantum chemical calculations for the (3^1 *R*) or (3^1 *S*) stereoisomers using methanol as a fifth ligand. The Mg ion can be positioned at the same side of the porphyrin plane as the 17^1-C (*syn*) or at the opposite side (*anti*). The two energetically most favorable forms are the (3^1 *R*)-*anti* and the (3^1 *S*)-*syn* combinations. Stacks of molecules of the *syn* or *anti* type can be formed by successive coordination of the 3^1-OH to the Mg of the next molecule (Fig. 6). From model studies, it was concluded that the ratio between the two stereoisomers can vary considerably. Provided a minor fraction of either form is present, the rods can be formed (Steensgaard et al., 2000). This suggests that both species can be accommodated in a stack by rotating the 3-side chain.

The stacks can be combined to form layers by hydrogen bonding between the 3^1-OH groups of one stack with the 13^1-C=O of a neighboring stack. Evidence for this has also been found by ^{13}C CP/MAS experiments. From the CP build-up of the 13^1-carbon signal in the chlorosomes of *Cfl. aurantiacus* and in the hexane treated aggregate, it was concluded that the 13^1 carbonyl is hydrogen bonded, probably to the 3-hydroxyethyl group (Nozawa et al., 1990).

Based on the NMR results, a bilayer tube model was proposed for the chlorosome rods in *Chl. tepidum*, where a predominantly *syn* layer forms the inner tube with the tails filling the center, while a layer of *anti* character constitutes the outer tube with the tails pointing away from the surface (Fig. 6) (van Rossum et al., 2001). In the *anti* conformation, the layer of BChls corresponds to the model of Holzwarth et al., where the tails are directed outward (Holzwarth and Schaffner, 1994). The layer formed from *syn* stacks has an opposite curvature with the tails directed inward. The existence of two different parallel chain stacks with *syn* and *anti* configurations has also been detected by NMR in solution (Mizoguchi et al., 1998). The two different layers (Fig. 6) have virtually identical aggregation shifts. Evidently, the overlap in both cases is similar and induces the same ring current shifts. The bilayer model is supported by electron microscopy, since the rod-shaped structures with an outer diameter of 10 nm and an internal hole of 3 nm (Cruden and Stanier, 1970; Staehelin et al., 1980) can be formed easily from the bilayer tube inferred from the MAS NMR data. Calculations of optical spectra based on a single outer layer at least explain the measured spectra satisfactorily, and refinements including the bilayer are expected (Prokhorenko et al., 2000; Psencik et al., 2003).

For the bilayer tubes, an intensity ratio between components **I** and **II** of approx. 3:2 is observed (van

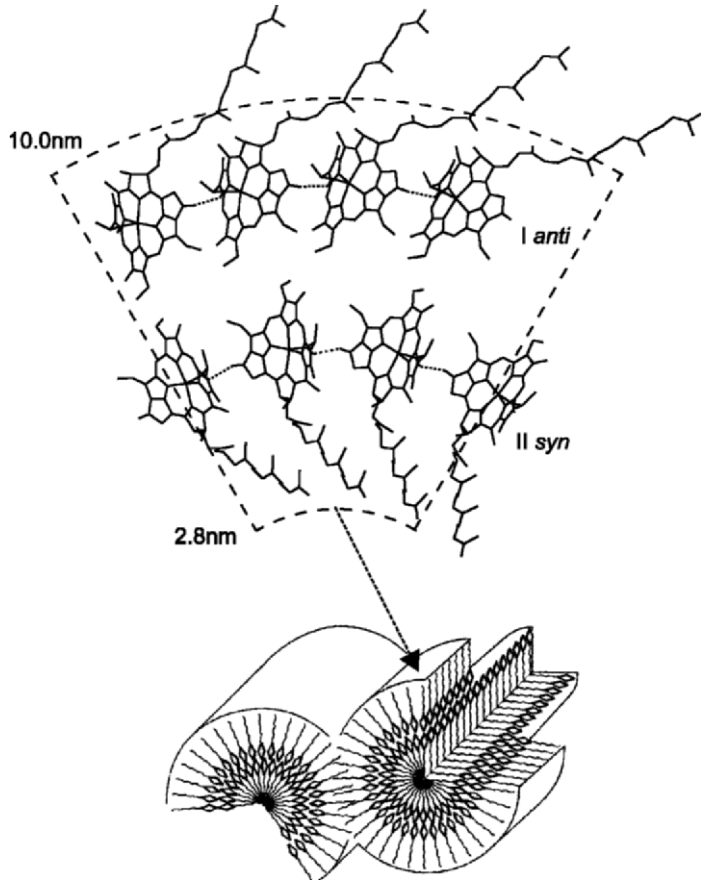

Fig. 6. Schematic representation of a radial wall section of a bilayer tube formed from curved 2-D sheets of *anti* (**I**) and *syn* (**II**) stacks. The chlorin rings are completed with the farnesyl tails, which were not included in the *ab initio* calculations. The curvature leads in a natural way to the dimensions determined with electron microscopy. The direction of the stacks is perpendicular to the plane of the paper. The dotted lines indicate hydrogen bonds between 13^1-C=O and 3^1-OH of adjacent stacks. In reality, the interface between the outer and inner tube is expected to be more dense than in this schematic representation, to account for the aggregation shifts of the 7^1 methyls.

Rossum et al., 2001). The splitting of the chemical shift pattern was explained by an interaction between *syn* and *anti* layers yielding a different electronic environment. The component **I** in the NMR spectra was attributed to a (3^1 *R*) *anti* structure and the component **II** to a (3^1 *S*) *syn* structure. The upfield shifts around the 7^1-CH_3 in component **II** may reflect a different structural arrangement for the 7-Me groups at the interface of the layers leading to an extended overlap for this component only. Finally, comparison of the proton responses of the farnesyl chain of BChl *c* with the phytyl chain of self-aggregated Chl *a*/H_2O reveals a significant excess line broadening of the BChl *c* proton signals, suggesting that the farnesyl chain may exhibit some random folding. On the other hand, it was demonstrated that the NMR relaxation parameters of the farnesyl chain are highly similar to those of the rigid ring system, from which it was concluded that at least a substantial fraction of the farnesyl chains should be relatively immobile (van Rossum et al., 1998b). This is consistent with the bilayer tube model of Fig. 6, since it can be expected that at least the fatty tails on the inside will be rigidly held in place.

V. Conclusions and Future Prospects

With a combination of chemical shift data and intermolecular constraints, detailed information about the structure of chlorosomes and solid chlorophyll aggregates can be obtained. Access to the proton chemical shifts in the solid state yields aggregation shifts that can be related to the stacking of the mac-

rocycles. The intermolecular correlations provide direct structural information in terms of close contacts between molecules. A few contacts strongly reduce the number of possible space filling arrangements for the chlorophyll aggregates.

For the study of the chlorosomes, MAS NMR has proved to be a valuable tool, and the model structure of Fig. 6 is increasingly accepted (Brown and Spiess, 2001; Glaeser et al., 2002; Vassilieva et al., 2002). MAS NMR in conjunction with other spectroscopic methods and microscopy provide converging evidence for the bilayer tube model of Fig. 6. The aggregation shift pattern in the 7-C region of component II in Fig. 4 was not yet explained quantitatively from the model structure. In addition, the large shift for the 5-C is not yet fully clear.

One key issue to be addressed in the near future is to prove that specific side chains can steer the supramolecular structure through the aggregation process. In particular, the role of the (3^1 *R*) and (3^1 *S*) stereoisomers, the long ester tails and their interplay appears to be important. It is expected that MAS NMR will contribute in the near future by resolving the structures of model compounds and other chlorosomes such as those found in *Chloroflexus*.

More material is available on the web, see [WEBSITE]. This includes a section describing the MAS NMR methods for structure determination. In addition, the web section includes tables with the ^{1}H and ^{13}C chemical shifts for solid Chl *a*/H_2O and BChl *c* as well as the aggregation shifts relative to the shifts in solution.

Note Added in Proof

To investigate the molecular control over the supramolecular structure, two model cadmium chlorins were studied that were uniformly ^{13}C and ^{15}N enriched in the ring moieties (de Boer et al., 2003, 2004). The chlorin models differ from the natural BChl *c* in the central metal and the 3-, 12-, 17-, and 20-side chains. One model system has the farnesyl tail replaced by a methyl, whereas the other has a stearyl tail. The ^{113}Cd MAS NMR signals reveal a five-coordination of the Cd metal, very similar to the HO•••Mg coordination in the natural system. Large ^{1}H ring-current shifts of up to 10 ppm reveal a dense orderly stacking of the molecules in planar layers, for which a correlation length of at least 24 Å was defined from long-range ring-current shift calculations (de Boer et al., 2004). The ring current shift calculations are a critical assay in discriminating between tubular and planar structures, since they can be applied to confront models deduced from e.g., electron microscopy with the NMR spectroscopy data from intact chlorosomes. The model structures confirm and validate the essential role of the [3^1R] and [3^1S] stereoisomers in the formation of the chlorosomal antennae. The 3D arrangement of the layers is revealed by intermolecular ^{13}C-^{13}C correlations obtained from CHHC experiments. With the tail truncated to methyl, a microcrystalline solid is formed with favorable interactions between the planar sheets in a head-to-tail orientation. The stearyl tails lead to a considerably disordered aggregate consisting of both *syn* and *anti* layers similar to the chlorosomes, as indicated by a doubling of the ^{15}N-D NMR signal. The MAS results provide converging evidence for a balance between strong local interactions and contributions to the free energy of the system associated with a longer length scale. The metal coordination and hydrogen bonding between stacks lead to a robust layer structure on a mesoscopic length scale, stable against thermodynamic noise. This allows for fine-tuning of the structure by various microscopic functionalities. The chirality of 3^1 side chain provides a bias for the two opposite plane curvatures, while bulky side chains like the 20 methyl provide fine tuning of the π-π overlap between individual macrocycles (de Boer et al., 2004). Finally the long tails promote an organization into bilayers with a 180° screw axis between the layers (de Boer et al., 2003).

Note: Readers are encouraged to visit the website (http://epub.ub.uni-muenchen.de/archive/00000776/) for 'supplementary material,' where Figs. S1–S2 referred to in the text are posted.

References

Abraham RJ and Rowan AE (1991) Nuclear magnetic resonance spectroscopy of chlorophyll. In: Scheer H (ed) Chlorophylls, pp 797–834. CRC Press, Boca Raton

Balaban TS, Holzwarth AR, Schaffner K, Boender GJ and de Groot HJM (1995) CP-MAS C-13-NMR Dipolar correlation spectroscopy of C-13-enriched chlorosomes and isolated bacteriochlorophyll *c* aggregates of *Chlorobium tepidum*: The self-organization of pigments is the main structural feature of chlorosomes. Biochemistry 34: 15259–15266

Bäuerlein E (2003) Biomineralization of unicellular organisms: An unusual membrane biochemistry for the production of

inorganic nano- and microstructures. Angew Chem Intl Ed 42: 614–641

Blankenship RE, Olson JM and Miller B (eds) (1995) Anoxygenic Photosynthetic Bacteria. Kluwer Academic Publishers, Dordrecht

Boender GJ (1996) The stacking of chlorophylls in the chlorosomal antennae of green bacteria. PhD Thesis. Leiden University. Leiden

Boender GJ, Raap J, Prytulla S, Oschkinat H and de Groot HJM (1995) MAS NMR structure refinement of uniformly C-13 enriched chlorophyll-*a* water aggregates with 2D dipolar correlation spectroscopy. Chem Phys Lett 237: 502–508

Brown SP and Spiess HW (2001) Advanced solid-state NMR methods for the elucidation of structure and dynamics of molecular, macromolecular, and supramolecular systems. Chem Rev 101: 4125–4155

Chiefari J, Griebenow K, Griebenow N, Balaban TS, Holzwarth AR and Schaffner K (1995) Models for the pigment organization in the chlorosomes of photosynthetic bacteria — diastereoselective control of in-vitro bacteriochlorophyll c_s aggregation. J Phys Chem 99: 1357–1365

Cruden DL and Stanier RY (1970) The characterization of *Chlorobium* vesicles and membranes isolated from green bacteria. Arch Microbiol 72: 115–134

de Boer I, Bosman L, Raap J, Oschkinat H and de Groot HJM (2002) 2D C-13-C-13 MAS NMR correlation spectroscopy with mixing by true 1H spin diffusion reveals long-range intermolecular distance restraints in ultra high magnetic field. J Magn Reson 157: 286–291

de Boer I, Matysik J, Amakawa M, Yagai S, Tamiaki H, Holzwarth AR and de Groot HJM (2003) MAS NMR structure of a microcrystalline Cd-bacteriochlorophyll *d* analoge. J Am Chem Soc 125: 13374–13375

de Boer I, Matysik J, Erkelens K, Sasaki S, Miyatake T, Yagai S, Tamiaki H, Holzwarth AR and de Groot HJM (2004) MAS NMR structures of aggregated cadmium chlorins reveal molecular control of self-assembly of chlorosomal bacteriochlorophylls. J Phys Chem B 108: 16556–16566

Glaeser J, Baneras L, Rutters H and Overmann J (2002) Novel bacteriochlorophyll *e* structures and species-specific variability of pigment composition in green sulfur bacteria. Arch Microbiol 177: 475–485

Griebenow K, Holzwarth AR, van Mourik F and van Grondelle R (1991) Pigment organization and energy-transfer in green bacteria. 2. Circular and linear dichroism spectra of protein-containing and protein-free chlorosomes isolated from *Chloroflexus aurantiacus* strain Ok-70-Fl. Biochim Biophys Acta 1058: 194–202

Hildebrandt P, Tamiaki H, Holzwarth AR and Schaffner K (1994) Resonance Raman-spectroscopic study of metallochlorin aggregates — implications for the supramolecular structure in chlorosomal BChl *c* antennae of green bacteria. J Phys Chem 98: 2192–2197

Holzwarth AR and Schaffner K (1994) On the structure of bacteriochlorophyll molecular aggregates in the chlorosomes of green bacteria — a molecular modeling study. Photosynth Res 41: 225–233

Katz JJ, Bowman MK, Michalski TJ and Worcester DL (1991) Chlorophyll aggregation: Chlorophyll/water micelles as models for in vivo long-wavelength chlorophyll. In: Scheer H (ed) Chlorophylls, pp 211–235. CRC Press, Boca Raton

Matsuura K, Hirota M, Shimada K and Mimuro M (1993) Spectral forms and orientation of bacteriochlorophyll-*c* and bacteriochlorophyll-*a* in chlorosomes of the green photosynthetic bacterium *Chloroflexus aurantiacus*. Photochem Photobiol 57: 92–97

Mizoguchi T, Sakamoto S, Koyama Y, Ogura K and Inagaki F (1998) The structure of the aggregate form of bacteriochlorophyll *c* showing the Q(y) absorption above 740 nm as determined by the ring-current effects on H-1 and C-13 nuclei and by H-1-H-1 intermolecular NOE correlations. Photochem Photobiol 67: 239–248

Nozawa T, Manabu S, Kanno S and Shirai S (1990) CP/MAS C-13-NMR Studies on the structure of bacteriochlorophyll *c* in chlorosomes from *Chloroflexus aurantiacus*. Chem Lett 1990: 1805–1808

Nozawa T, Suzuki M, Ohtomo K, Morishita Y, Konami H and Madigan MT (1991) Aggregation structure of bacteriochlorophyll *c* in chlorosomes from *Chlorobium tepidum*. Chem Lett 1991: 1641–1644

Nozawa T, Ohtomo K, Suzuki M, Nakagawa H, Shikama Y, Konami H and Wang ZY (1994) Structures of chlorosomes and aggregated BChl *c* in *Chlorobium tepidum* from solid state high resolution CP/MAS C-13 NMR. Photosynth Res 41: 211–223

Olson JM (1998) Chlorophyll organization and function in green photosynthetic bacteria. Photochem Photobiol 67: 61–75

Prokhorenko VI, Steensgaard DB and Holzwarth AR (2000) Exciton dynamics in the chlorosomal antennae of the green bacteria *Chloroflexus aurantiacus* and *Chlorobium tepidum*. Biophys J 79: 2105–2120

Psencik J, Ma YZ, Arellano JB, Hala J and Gillbro T (2003) Excitation energy transfer dynamics and excited-state structure in chlorosomes of *Chlorobium phaeobacteroides*. Biophys J 84: 1161–1179

Staehelin LA, Golecki JR, Fuller RC and Drews G (1978) Visualisation of the supramolecular architecture of chlorosomes (*Chlorobium* type vesicles) in freeze-fractured cells of *Chloroflexus aurantiacus*. Arch Mikrobiol 119: 269–277

Staehelin LA, Golecki JR and Drews G (1980) Supramolecular organization of chlorosomes (*Chlorobium* vesicles) and of their membrane attachment sites in *Chlorobium limicola*. Biochim Biophys Acta 589: 30–45

Steensgaard DB, Wackerbarth H, Hildebrandt P and Holzwarth AR (2000) Diastereoselective control of bacteriochlorophyll *e* aggregation. 3(1)-S-BChl e is essential for the formation of chlorosome-like aggregates. J Phys Chem B 104: 10379–10386

Tamiaki H, Amakawa M, Holzwarth AR and Schaffner K (2002) Aggregation of synthetic metallochlorins in hexane. A model of chlorosomal bacteriochlorophyll self-assemblies in green bacteria. Photosynth Res 71: 59–67

Umetsu M, Wang ZY, Zhang J, Ishii T, Uehara K, Inoko Y, Kobayashi M and Nozawa T (1999) How the formation process influences the structure of BChl *c* aggregates. Photosynth Res 60: 229–239

Umetsu M, Hollander JG, Matysik J, Wang ZY, Adschiri T, Nozawa T and de Groot HJM (2004) Magic-angle spinning NMR under ultra-high field reveals two forms of intermolecular interaction within CH_2Cl_2-treated 3(1)-R-type bacteriochlorophyll *c* solid aggregate. J Phys Chem B 108: 2726–2734

van Rossum BJ, Boender GJ and deGroot HJM (1996) High magnetic field for enhanced proton resolution in high- speed CP/MAS heteronuclear H-1-C-13 dipolar-correlation spectros-

copy. J Magn Reson Ser A 120: 274–277

van Rossum BJ, Boender GJ, Mulder FM, Raap J, Balaban TS, Holzwarth A, Schaffner K, Prytulla S, Oschkinat H and de Groot HJM (1998a) Multidimensional CP-MAS C-13 NMR of uniformly enriched chlorophyll. Spectrochim Acta A54: 1167–1176

van Rossum BJ, Van Duyl BY, Steensgaard DB, Balaban ST, Holzwarth AR, Schaffner K and De Groot HJM (1998b) Evidence from solid state NMR dipolar correlation spectroscopy for dual interstack arrangements in the chlorosome antenna system. In: Garab G (ed) Photosynthesis: Mechanisms and Effects, pp 117–120. Kluwer Academic Publishers, Dordrecht

van Rossum BJ, Steensgaard DB, Mulder FM, Boender GJ, Schaffner K, Holzwarth AR and de Groot HJM (2001) A refined model of the chlorosomal antennae of the green bacterium *Chlorobium tepidum* from proton chemical shift constraints obtained with high-field 2-D and 3-D MAS NMR dipolar correlation spectroscopy. Biochemistry 40: 1587–1595

van Rossum BJ, Schulten EAM, Raap J, Oschkinat H and de Groot HJM (2002) A 3-D structural model of solid self-assembled chlorophyll *a*/H_2O from multispin labeling and MAS NMR 2-D dipolar correlation spectroscopy in high magnetic field. J Magn Reson 155: 1–14

Vassilieva EV, Stirewalt VL, Jakobs CU, Frigaard NU, Inoue-Sakamoto K, Baker MA, Sotak A and Bryant DA (2002) Subcellular localization of chlorosome proteins in *Chlorobium tepidum* and characterization of three new chlorosome proteins: CsmF, CsrnH, and CsmX. Biochemistry 41: 4358–4370

Worcester DL, Michalski TJ and Katz JJ (1986) Small-angle neutron scattering studies of chlorophyll micelles: Models for bacterial antenna chlorophyll. Proc Natl Acad Sci USA 83: 3791–3795